2007

Magnetite (Fe3O4): Properties, Synthesis, and Applications

Lee Blaney

Magnetite: Properties, Synthesis, & Application

Lee Blaney

SYNOPSIS

The subsequent report presents scientific data concerning properties of micro- (diameter in 10^{-6} m meter range) and nano- (diameter in 10^{-9} m meter range) magnetite, an iron oxide with chemical structure Fe_3O_4, particles; additionally, the properties of nano-particulate magnetite are discussed in regards to potential applications in environmental engineering, biomedical/medical, microfluidic, and mechano-electrical fields.

Nano-scale magnetite particles are approximately one billion times smaller (by volume) than micro-scale magnetite particulates and exhibit much different properties. Producing particles of such small size is extremely difficult for numerous reasons; however, various methods have been documented in the open literature. These methods involve (a) thermo-chemical precipitation reactions in solution, or (b) chemical reactions in specialized "reactors."

As mentioned above, nano-scale magnetite provides exciting opportunities in a number of fields; these potential applications are summarized below:

- **High Gradient Magnetic Separation:** environmental engineering has traditionally dealt with removing particles and contamination from drinking/waste water streams. Nano-scale magnetite particles can bind

(through electro-chemical interaction) with suspended particles and settle as sludge; subsequently, magnetite nanoparticles can be recycled through utilization of a magnetic field recovery system. Radioactive chemicals and toxic/carcinogenic metals can also be removed using nano-magnetite.

- **Magnetic Resonance Technology:** when a person receives an MRI, doctors take an image that helps them to locate abnormalities in the human body's tissue or organs. Magnetite nanoparticles offer potential for clearer imaging of such tissue and organs; furthermore, nano-magnetite can be modified to allow for organ-specific imaging.
- **Drug Delivery:** scientists are now trying to develop mechanisms that allow drugs to go directly to a certain area of the human body. For instance, if someone has liver cancer and a drug has been developed to combat such disease, the drug can be attached to magnetite nanoparticles through a series of methods, then the nano-magnetite can be delivered directly to the liver and the drug can be released.
- **Other:** low-friction seals, dampening and cooling agents in loudspeakers, magnetically active membrane biological reactor, regenerant solution, recovery of hazardous wastes, and controlled microfluidic flow.

Clearly, nano-scale magnetite offers potential for creation of novel technology in multiple fields of study. The following report will shed more light on production methods, nano-scale properties, and applications.

LIST OF TERMS & VARIABLES

Symbol	Description
a	lattice parameter
CFSE	crystal field stabilization energy
d	particle diameter
EPMA	electron probe microanalysis
Ferrous	reduced iron species, Fe^{2+}
Ferric	oxidized iron species, Fe^{3+}
Fe_3O_4	chemical formula for magnetite
γ	surface tension
HGMS	high gradient magnetic separation
∞	bulk phase
l	liquid phase
L	molar heat of fusion
MBR	membrane biological reactor
MRI	magnetic resonance imaging
MRT	magnetic resonance tomography
v	specific molar volume
P	pressure
PEO	polyethylene oxide
$P_{Laplace}$	Laplace pressure
r	particle radius
s	solid phase
T_m	melting temperature
VTT	Verwey transition temperature
XRD	x-ray diffraction
z	number of unit cells in a formula unit of magnetite

1 INTRODUCTION

Utilization of magnets as navigational devices extends back to 8th century China; however, natural magnets, nicknamed loadstones, have been employed as fortune-telling devices since 200 B.C. (Mills, 2004). Natural organisms, known as magnetotactic bacteria, have been using nano-scale (30-100 nm) magnetic particles since ancient times in order to orient and migrate along geomagnetic fields towards favorable habitats (Blakemore, 1982). Magnetic particles utilized by Chinese sailors and magnetotactic organisms are chemically composed of Fe_3O_4, or magnetite; "magnetite," derives from the district of Magnesia in Asia Minor, where large deposits of magnetite were discovered (Bellis, 2006). Containing both ferrous (reduced) and ferric (oxidized) iron species, magnetite is oftentimes described as $iron^{II,III}$ oxide. An oversimplified synthesis reaction (Figure 1) demonstrates the chemical makeup of the compound:

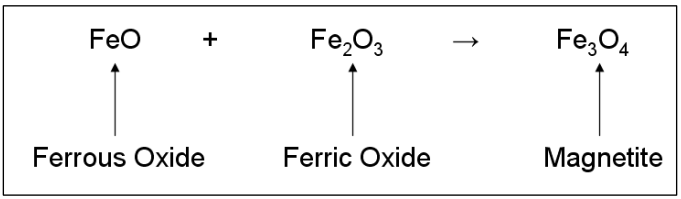

Figure 1. Oversimplified magnetite synthesis reaction

This naturally occurring magnetic compound clearly contains many interesting properties and potential for various applications. The ensuing report describes properties of bulk magnetite, illustrates techniques for synthesizing nano-scale magnetite particles, explains properties (of interest) of these nanoparticles, and discusses various applications for which nano-scale magnetite particles may be successfully utilized.

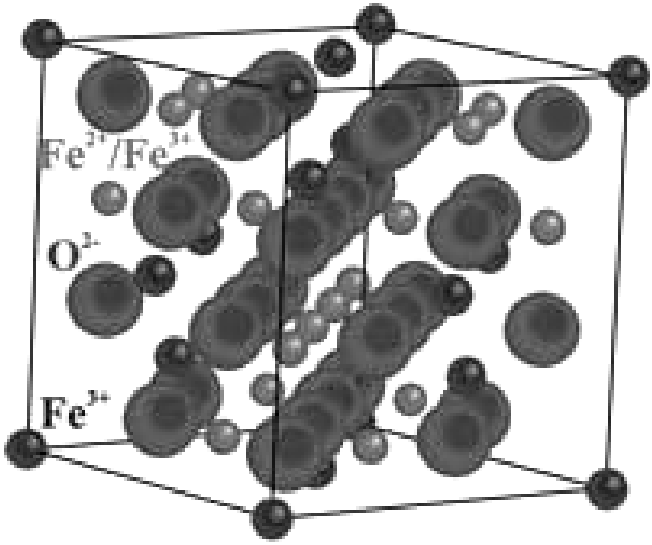

Figure 2. Structure and Unit Cell of Magnetite

2 BULK PROPERTIES

This section will explore the bulk properties (physical, structural, thermal, electrical, and magnetic) of magnetite. Section three of this report will detail the properties of nano-scale magnetite; undoubtedly, only nano-properties of importance (i.e., magnetic) will be available in the literature. Regardless, extensively documented bulk properties will be presented towards relation with various synthesis techniques, nano-scale properties or applications. For summarized magnetite properties see Appendix A.

2.1 Structural Properties

Magnetite's crystal structure follows an inverse spinel pattern with alternating octahedral and tetrahedral-octahedra layers (Hill *et al*., 1979). From Figure 2, ferrous species are observed to occupy half of the octahedral lattice sites due to greater ferrous crystal field stabilization energy (CFSE); alternatively, ferric species occupy the other octahedral lattice

sites and all tetrahedral lattice sites (Cornell and Schwertmann, 1996). This preponderance allows for application of the chemical formula $Y[XY]O_4$, where brackets represent octahedral sites while the absence of brackets represents tetrahedral sites; consequently, X and Y symbolize ferrous and ferric, respectively (Cornell and Schwertmann, 1996). Additionally, magnetite unit cells adhere to the face-centered cubic pattern with crystal lattice parameter, $a = 0.8396$ nm (Cornell and Schwertmann, 1996). Moreover, Figure 2 demonstrates the presence of eight formula units (z parameter) within each magnetite unit cell.

Bulk magnetite particles exhibit twinning along {111} the plane (Kostov, 1968); cubic terracing occurs on the (100) face and atomically flat terracing, oriented along the main crystallographic direction, occurs on the (111) plane (Seoighe *et al*., 1999; Shackhutdinov and Weiss, 2000).

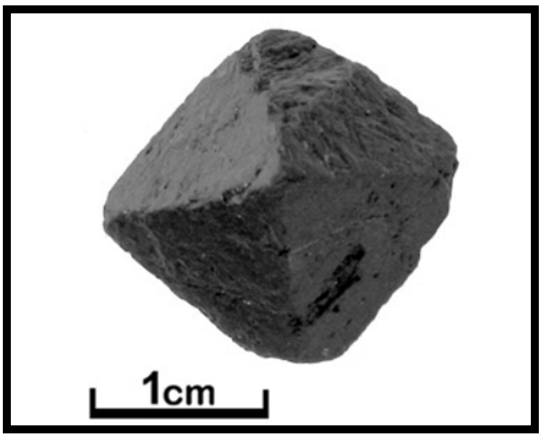

Figure 3. Example of macro-scale magnetite

2.2 Physical Properties

Natural and synthesized magnetite micro-scale crystals exhibit metallic luster and opaque jet black color, as illustrated in Figure 3. Magnetite's density is established at 5.18 g/cm^3, slightly lighter than reddish-brown hematite (α-Fe_2O_3; 5.26 g/cm^3) and somewhat heavier than yellowish-orange ferrihydrite (α-FeOOH; 4.26 g/cm^3); pure iron (α-Fe) has a density of 7.87 g/cm^3. At ambient temperatures, magnetite particles exhibit hardness of 5.5, identical to glass. (Cornell and Schwertmann, 1996)

Effective surface areas of magnetite vary according to synthesis method as certain procedures generate coarser/finer particles; however, typical micro-scale particles with approximate diameters of 0.2 μm exhibit surface areas of approximately 6 m^2g^{-1} (Mannweiler, 1966). Magnetite particles are not porous (Cornell and Schwertmann, 1996).

Standard Gibb's free energy of magnetite formation is -1012.6 kJ/mol; therefore, formation of magnetite is thermodynamically favorable (Cornell and Schwertmann, 1996). Additionally, the standard enthalpy and entropy of magnetite formation are -1115.7 kJ/mol and 146.1 kJ/mol/K, respectively (Robie *et al*., 1978; Hemingway, 1990).

Solubility products differ depending on the applicable dissolution reaction; however, generally speaking magnetite dissolution is much faster than other pure ferric oxides (Sweeton and Baes, 1970).

2.3 Thermal Properties

Magnetite melting/boiling points are observed at 1590 and 2623 °C, respectively. Heats of fusion, decomposition, and vaporization are 138.16, 605.0, and 298.0 kJ/mol (at 2623 °C), respectively. (Samsonov, 1973)

2.4 Electrical Properties

As mentioned earlier, octahedral sites in the magnetite structure contain ferrous and ferric species. The electrons coordinated with these iron species are thermally delocalized and migrate within the magnetite structure causing high conductivity exchange constants: ranging from -28 J·K to 3 J·K between tetrahedral/octahedral sites and octahedral/octahedral sites, respectively (Cornell and Schwertmann, 1996). Magnetite's Verwey transition temperature (VTT) (118 K) exhibits an ordered arrangement of ferrous and ferric ions on octahedral sites, inhibiting electron delocalization when temperatures fall below VTT (Cornell and Schwertmann, 1996). Furthermore, due to electron delocalization effects magnetite can be slightly metal deficient on octahedral sites; such deficiency allows for n- and p-type magnetite semiconductors (Cornell and Schwertmann, 1996).

Resultant conductivities range from 10^{2}–10^{3} $\Omega^{-1}cm^{-1}$ (Cornell and Schwertmann, 1996). Figure 4 demonstrates that such electrical conductivity evidence semi-conductor behavior; however, this conductivity range borders conductor (metallic) behavior. Metals, semiconductors, and insulators historically exhibit bandgaps ranging from 0.0, 0.2–3.0, >3.0 eV (Kiely, 2006). Semi-metallic behavior is further supported by magnetite's relatively low bandgap (0.1 eV) (Cornell and Schwertmann, 1996).

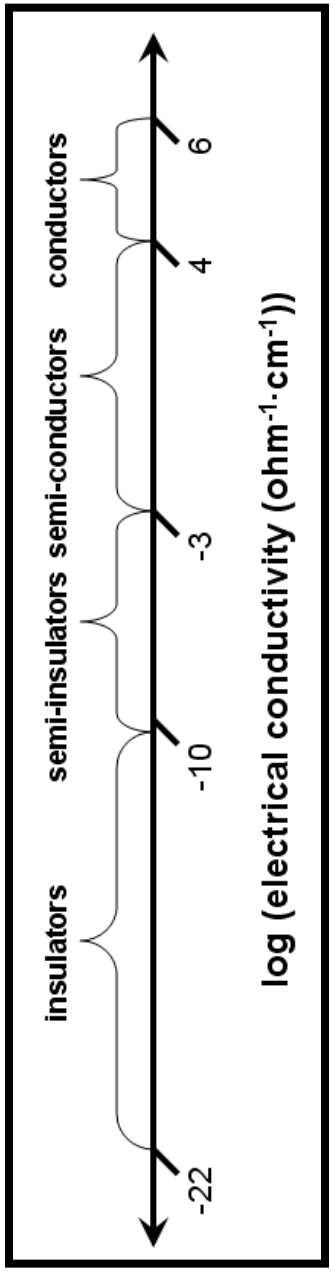

Figure 4: Electrical conductivity scale and resultant behavior

2.5 Magnetic Properties

Magnetite's Curie temperature is observed at 850 K. Below the Curie temperature, magnetic moments on tetrahedral sites, occupied by ferric species, are ferro-magnetically aligned while magnetic moments on octahedral sites, occupied by ferrous and ferric species, are antiferro-magnetic and cancel each other; such combined behavior is termed ferrimagnetic (Cornell and Schwertmann, 1996). Therefore, at room temperature, magnetite is ferrimagnetic. Figure 5 illustrates the ferro-magnetic behavior of tetrahedral sites and mentions the antiferro-magnetic behavior of octahedral sites.

As temperatures increase to the Curie temperature, thermal fluctuations destroy the ferromagnetic alignment of magnetic moments on tetrahedral sites; hence, ferrimagnetic strength is diminished. When the Curie temperature is attained, net magnetization becomes zero and superpara-magnetic behavior is observed.

Coercivity, the magnitude of applied magnetic field required for zero magnetization after magnetic saturation (determined from hysteresis loops, see Figure 10), can be controlled during magnetite precipitation reactions; coercivit-ties range from 2.4 (typical of disk drive recording media) to 20.0 (permanent magnet realm) kAm^{-1} (Meisen and Kathrein, 2000).

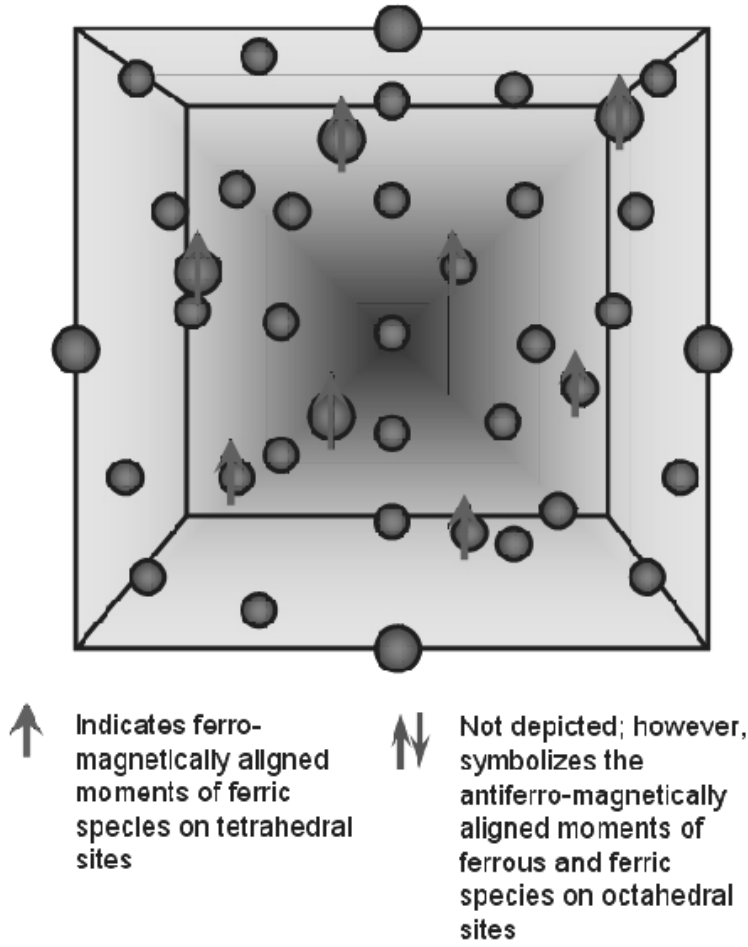

Figure 5:Ferrimagnetic behavior of magnetite

3 PROCEDURES FOR NANOPARTICLE SYNTHESIS

Within this section of the report several well-documented magnetite nanoparticle synthesis techniques will be discussed. While there are several distinct physico-chemical procedures to synthesize magnetite nanoparticles, the majority of these methods fall under two categories: polymer/surfactant

assisted precipitation reactions and co-precipitation reactions. Synthesis procedures of interest for this report include reverse micelle, copolymer gels, co-precipitation, solvothermal reduction, and ion exchange resin. The following subsections will provide brief descriptions of each method and a summary of relative advantages and disadvantages of select methods.

3.1 Reverse Micelle

The reverse micelle method is basically a water-in-oil emulsions that generate reverse micelles, which act as nano-reactors for various physico-chemical processes. In this particular case, a reverse micelle solution is created by inversion of typical surfactant micelles as illustrated below in Figure 6.

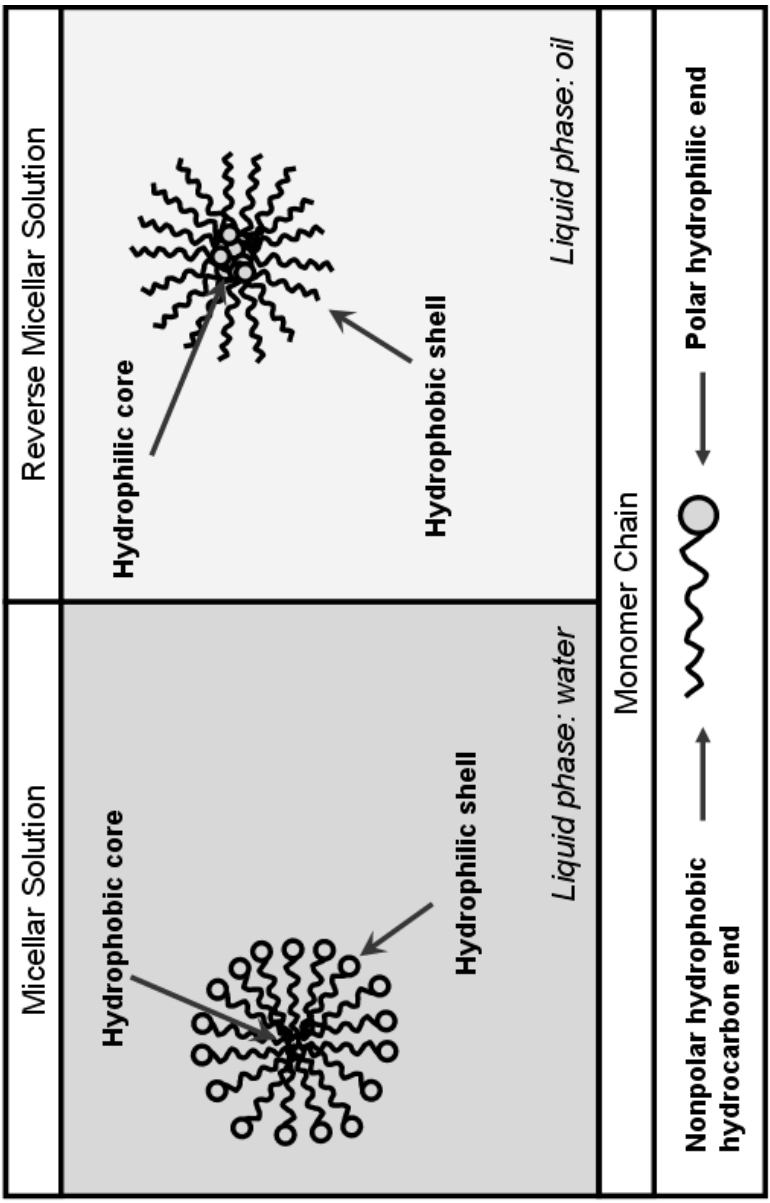

Figure 6: Schematic of Micelle and Reverse Micelle Solutions

As evidenced by the above illustration, micellar solutions can be utilized towards separation of hydrophobic compounds and subsequent precipitation of micellar units. Such processes are often employed in removal of suspended/colloidal particles in water treatment; accordingly, reverse micellar units could treat aqueous compounds. Through exploitation of this physico-chemical behavior, nanoreactors for aqueous compounds can be generated in the hydrophilic cores of reverse micelles. Dissolvable metal species (such as iron) partition into the aqueous phase (water-in-oil emulsions) contained within the reverse micellar cores. A nano-scale reactor containing the species of interest now exists at the reverse micelle center; this scenario allows for various chemical reactions to be realized within user-defined, alterable, dimensionally restricted spaces. Furthermore, simultaneous nanoparticle production and steric stabilization (through adsorption of surfactant monomers) can be realized.

Numerous reverse micelle methods and chemical protocols towards synthesis of magnetite nanoparticles have been documented in the literature (Fried *et al*., 2001; Tang *et al*., 2003; Zhou *et al*., 2001; Tartaj and Serna, 2002; Selim *et al*., 1997; Lee *et al*., 2005). The following procedure discusses generation of magnetite nanoparticles by Lee *et al*., who have detailed a synthesis protocol capable of producing monodispersed nanoparticles of uniform diameters over the 2-10 nm range (Lee *et al*., 2005). Nanoparticle diameter is governed by the relative amounts of surfactant and solvent and the ratio of polar solvent to surfactant.

Surfactant (dodecylbenzenesulfonate) is added to an oil (xylene) solution, creating an opaque solution. This solution is subsequently mixed through a sonication process, which bombards the sample with highly intensive ultrasonic waves and ultimately homogenizes the emulsion. An iron solution

containing 1:2 (molar ratio) ferrous to ferric species (ferrous chloride, ferric nitrate) in alcohol (ethanol) is vigorously stirred into the homogenized emulsion solution. Shortly thereafter (a few seconds), the opaque emulsion becomes transparent; after 12 hours of stirring, the reverse micelle phase (water-in-oil phase) stabilizes. Gradual heating of reverse micelle solutions to 90 °C under anoxic conditions (argon flow – towards prevention of ferrous oxidation) ensues. A strong reducing agent (hydrazine) is introduced to the system; immediately afterwards, the transparent solution turns black. Refluxing the solution and centrifugation in ethanol allowed magnetite nanoparticle recovery. Nanoparticles are readily dispersed in organic solvents (Lee *et al*., 2005) self-assemble into two-dimensional arrays out of solution (Fried *et al*., 2001).

3.2 Copolymer Templates

Employment of copolymer templates towards synthesis of various nanoparticles has been described in the literature (Breulmann *et al*., 1998; Morais *et al*., 2002; Lin *et al*., 2003; Suber *et al*., 2001; Rabelo *et al*., 2000). Copolymer templates are usually ion exchange resins; commonly observed examples include micro-scale styrene beads with divinylbenzene cross-linking. Resins are mesoporous (pore diameter ranging from 2-50 nm) and exude cation exchange capabilities (i.e., negatively charged functional groups, such as sulfonic groups, permit cation sorption/desorption). Figure 7 demonstrates the structure of such copolymer templates.

Immersion of these copolymer templates into solution containing strong (high valence state, large species size), positive electrolytes results in sorption of said electrolytes by sulfonic groups. Loading the resins, and concurrently resin pores, with ferrous iron species produces nanoreactors capable

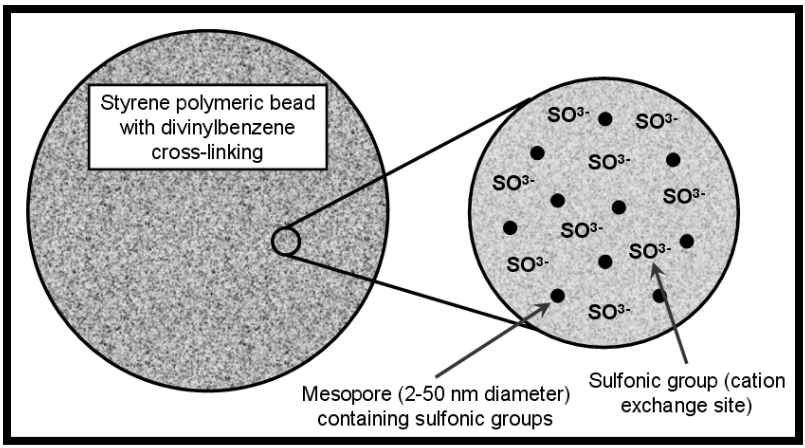

Figure 7: Schematic of mesoporous copolymer template containing cation exchange sites

of magnetite synthesis. Utilization of traditional micro-scale magnetite synthesis procedures in such systems results in precipitation of magnetite nanoparticles.

Numerous copolymer template procedures for synthesizing magnetite nanoparticles have been documented in the literature (Breulmann *et al*., 1998; Morais *et al*., 2002; Lin *et al*., 2003; Suber *et al*., 2001; Rabelo *et al*., 2000). Rabelo *et al*. have produced a straightforward protocol that utilizes the simple theory discussed above. Nanoparticle size control is governed by the concentration of ferrous ion incorporated into the polymeric template, due to mass-charging effects on sulfonic groups.

Rabelo *et al*.'s procedure calls for cation exchange polymeric resins containing sulfonic functional groups to be immersed into ferrous ($FeSO_4$) solution. The ferrous solution, containing polymeric beads, is stirred (one hour) at room temperature, promoting ferrous diffusion into resin pore

spaces and gel-phases; subsequently, resins are filtered and rinsed. Ferrous containing resins are then stirred into oxidizing solution (potassium hydroxide, sodium nitrate) maintained under anoxic conditions (nitrogen sparged) and 60 °C temperature. Note, a leading procedure towards synthesis of micro-scale magnetite particles involves similar techniques; however, instead of immersing ferrous-containing polymeric resins, ferrous salt is added directly. Resultant polymer supported magnetite nanoparticles are filtered, rinsed, and dried. (Rabelo *et al*., 2000)

3.3 Co-precipitation Reactions

Controlled co-precipitation techniques towards synthesis of magnetite nanoparticles are widespread and easily obtainable in the literature (Massart, 1981; Sahoo *et al*., 2001; Visalakshi *et al*., 1993; Kang *et al*., 1996; Tang *et al*., 2003; Qu *et al*., 1999). The chemical reaction utilized in these procedures involves alkinization of ferric and ferrous species. One major obstacle when employing such direct techniques is Oswald ripening, which is the phenomenon that causes aggregation of colloidal particles towards lower surface energy. Steric stabilization of suspended nanoparticles provides resolution of this problem.

Kim *et al*. describe one magnetite nanoparticle synthesis and stabilization procedure. Stock solution containing 1:2 (molar ratio) ferrous to ferric species (ferrous chloride, ferric chloride) was slowly poured (drop-wise) into alkali source, composed of sodium hydroxide, under vigorous stirring and nitrogen sparging. Magnetite crystals formed and precipitated; this powder was subsequently removed from solution through employment of an external magnetic field. The powder was subsequently rinsed with deionized water and separated via centrifugation; afterward, the powder underwent weak acid

rinse to neutralize anionic surface charges, again powders were separated via centrifugation. X-Ray Defraction (XRD) analysis demonstrated average particle diameters of 6 nm. Magnetite nanoparticles were then sterically stabilized using mechanically stirred sodium oleate solution (at weak base pH) at 90 °C temperature. (Kim *et al*., 2001)

Magnetite nanoparticle diameter control is provided by altering the sodium hydroxide concentration and pH. At constant pH, nanoparticle sizing is directly proportional to sodium hydroxide concentration; alternatively, when sodium hydroxide concentration is held constant, nanoparticle diameters are inversely proportional to pH. Therefore, smaller nanoparticles (diameter < 3 nm) are synthesized at higher pH and lower sodium hydroxide concentrations.

3.4 Other Chemical Techniques

Although the literature describes numerous techniques to synthesize magnetite nanoparticles, this report only details the theory and process dynamics for those listed above. Some other synthesis methods available through the literature include solvothermal reduction and thermal decomposition (Hou *et al*., 2003; Sapieszko and Matijevic, 1980; Woo *et al*., 2004; Sun and Zeng, 2002). These alternative synthesis processes are discussed in Appendix B.

3.5 Comparison of Synthesis Methods

Based on the above descriptions of various means of generating nano-scale magnetite particles, advantages and disadvantages with each process can be understood. Clearly, these advantages or disadvantages will dictate employment of nanoparticles towards various applications and settings.

If monodispersed, well-ordered, uniformly sized, magnetite nanoparticles are necessary for a given operation,

reverse micelle method provides excellent control over the synthesis process. Simple alteration of surfactant and solvent concentrations/volumes allows for tight control over nanoparticle diameter. Conversely, monodispersed, stabilized nanoparticles cannot be utilized in many applications because of pressure drop concerns (i.e., clogging). Copolymer templates allow for structural stability of magnetite nanoparticles through polymeric supports; however, nanoparticles are then removed from colloidal-phase to solid-phase, eliminating many potential employment capabilities in biomedical applications. Uniform sizing of copolymer embedded nanoparticles is operationally simple as varying of ferrous ion incorporation into polymeric templates allows for particle size control. Controlled co-precipitation, solvothermal reduction, and thermal decomposition, like reverse micelle procedures, allow for uniform nanoparticle sizing depending upon chemical concentrations; however, these reactions appear to be more operationally complex (variations in chemical conditions can be very sensitive) and thus deficient as compared to reverse micelle method.

Therefore, for applications requiring monodispersed, uniformly sized, stable magnetite nanoparticles, reverse micelle method is recommended; for applications entailing field operation (such as environmental remediation projects – see section five), copolymer template method is suggested to ensure synergy of polymeric rigidity and nano-scale magnetite chemico-magnetic properties.

4 PROPERTIES OF NANO-SCALE MAGNETITE

In section two of this report, "Bulk Properties of Magnetite," various structural, physical, thermal, electrical, and magnetic properties of magnetite were discussed. As magnetite particle diameters are decreased to the nano-scale,

structural, physical, thermal, electrical, and magnetic properties of begin to change. Many of these characteristic changes are thoroughly described in the literature (Thapa *et al*, 2004; Cornell and Schwertmann, 1996; Mannweiler, 1966; Pawlow, 1909; Kiely, 2006); however, the majority of nano-scale magnetite properties have not yet been explored. Obviously, a metal oxide named "magnetite" is not going to be utilized for advanced, state-of-the-art electronic or thermal applications. Consequently, little research has been published regarding various properties recorded in section two.

Regardless of the lack of overarching nanoparticle characterization, several properties have been experimentally determined. The following subsections will provide details about these property transitions from bulk- to nano-scale particles.

4.1 Structural Properties

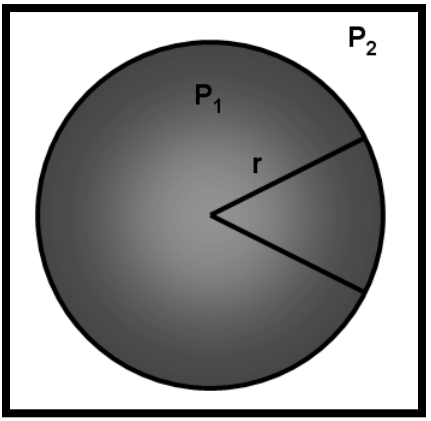

Figure 8. Effect of radius on Laplace pressure

Scanning electron microscopy analyses by Thapa *et al*. indicate that as magnetite particle size is decreased into the

nano-scale, the corresponding lattice parameter increases (Thapa *et al*, 2004). Understanding of this volume increase stems from fundamental surface chemistry relationships. Consider Figure 8, which illustrates a generic magnetite particle with radius, r, internal pressure, P_1, and external pressure, P_2.

Laplace determined that pressure variables are inversely related to particle radius and directly related to surface tension, as described below (Equation 1).

$$P_1 - P_2 = P_{Laplace} = \frac{2\gamma}{r} \qquad (Equation\ 1)$$

As particle radius decreases, Laplace pressure increases, effectively reducing the external pressure exerted on the particle. Lower external pressures result in particle swelling, which consequently causes unit cell expansion. Table 1 demonstrates lattice parameter and unit cell volume expansion between bulk magnetite and 6.4 nm particles. Unit cell bulging attributable to fluctuations in Laplace pressure are clearly observed. Regardless of this swelling, nano-scale magnetite still exhibits a face-centered cubic unit cell.

Table 1. Bulk vs. nano-scale unit cell dimensions (Cornell and Schwertmann, 1996; Thapa et al., 2004)

Material	Lattice parameter (Å)	Unit cell volume (Å^3)
Bulk magnetite	8.39	590.6
6.4 nm magnetite	8.40	592.7

Crystal structure of nano-scale magnetite remains constant; however, electron probe analyses imply that oxygen concentrations within magnetite particles decline as particle size is reduced. Consequently, a relative decrease in iron valence is observed, generating greater ferrous ion presence. This structural change is insignificant to structural properties of magnetite; however, some effect is observed on magnetic properties.

No information regarding twinning, parting, or terracing on magnetite nanoparticle surfaces could be gathered.

4.2 Physical Properties

In accord with many classroom discussions and examples, the effective surface area of nano-magnetite should increase with decreasing particle size. Figure 9 demonstrates the theory of this supposition.

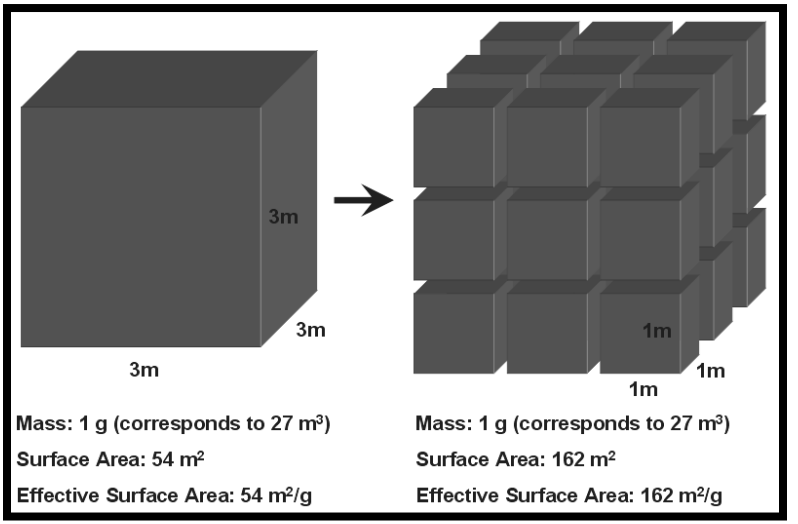

Figure 9. Increasing effective surface area with decreasing particle size.

Section two recorded micro-scale magnetite (0.2 μm) effective

surface area as 6 m^2g^{-1} (Mannweiler, 1966); conversely, effective surface areas of magnetite nanoparticles (~50 nm diameter) have been determined as approximately 100 m^2g^{-1} (Cornell and Schwertmann, 1996).

Colloidal magnetite solutions are typically characterized by the jet black color, hence no color change between bulk-scale and nano-scale magnetite is observed. Unit cell swelling should cause subsequent reduction in density; however, no experimental data confirming this assumption was located. Magnetite nano-particles are assumed nonporous. No information regarding hardness, free energy, or solubility of magnetite nanoparticles could be gathered.

4.3 Thermal Properties

In 1909, Iwan Petrowitsch Pawlow predicted that decreasing particle diameter should generate lower melting points, according to Equation 2 (Pawlow, 1909).

$$\frac{T_m(r)}{T_m(\infty)} = 1 - \frac{4\upsilon_s^{2/3}}{L}\left(\gamma_s \cdot 2\upsilon_s^{2/3} - \gamma_l \cdot 2\upsilon_l^{2/3}\right) \cdot \frac{1}{d}$$

(Equation 2)

Where T_m, ν, L, γ, d, s, l, and ∞ represent melting temperature, specific molar volume, molar heat of fusion, surface tension, particle diameter, solid phase, liquid phase, and bulk phase, respectively. No information regarding magnetite's surface tension could be found towards utilization of Pawlow's equation; however, a decline in melting/boiling temperatures of nano-scale magnetite can be assumed.

No information regarding heats of fusion, decomposition, or vaporization of magnetite nanoparticles could be gathered; however, as reduction in melting point is established, subsequent reduction in heats of fusion, decomposition, or vaporization can be deduced through logic and comparison with other materials (Schmidt *et al*., 1997).

4.4 Electrical Properties

No information regarding electrical properties of magnetite nanoparticles could be found in the literature. However, information regarding electrical conductivity and resistivity of polymer impregnated with magnetite particles was discovered; as this information relates to the copolymer template synthesis procedure, it will be presented herein. Magnetite incorporation into polymeric substances causes resistivity modification from insulator realm (0 vol% magnetite) to semi-conductor regime (10 kΩ·m at 47 vol% magnetite) (Weidenfeller *et al*., 2002).

4.5 Magnetic Properties

Section two describes the magnetization of bulk magnetite as ferrimagnetic, generated by parallel alignment of magnetic moments on tetrahedral sites and anti-parallel alignment of ferrous and ferric spins on octahedral sites. Typical ferrimagnetic behavior exerts coercivity and remanence (retentivity) as displayed in Figure 10. As particle size is decreased, the amount of exchange-coupled spins resisting spontaneous magnetic reorientation is decreased, tending towards paramagnetic or superparamagnetic magnetization (Kiely, 2006). Consequentially, decreasing magnetite particle size should demonstrate reduced ferrimagnetic and enhanced superparamagnetic behavior. Similarly, increasing temperatures enhance thermal energy of

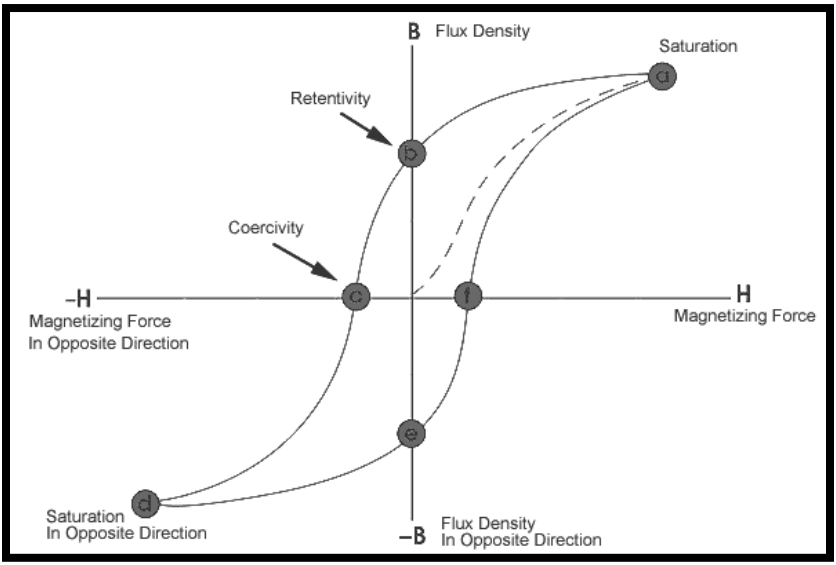

Figure 10. Generic ferrimagnetic hysteresis loop

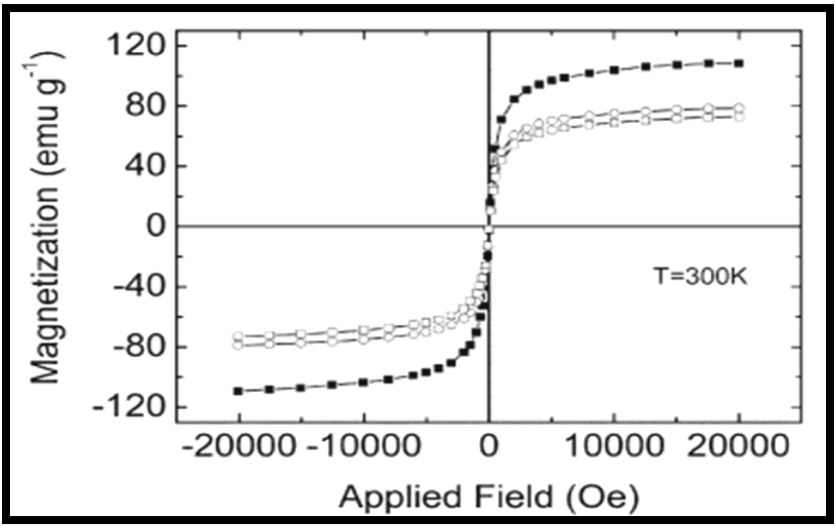

Figure 11. Absence of hysteresis loop (for three different particles) implies superparamagnetism (Hou et al., 2003)

particles and thus facilitate magnetic reorientation, or superparamagnetic magnetization (Kiely, 2006). In accordance with superparamagnetic behavior, magnetite nanoparticles exhibit zero coercivity and remanence in hysteresis loops as illustrated in Figure 11. Coercivity slowly builds as magnetite particle diameter increases.

Reduction in particle size also affects the Curie temperature, which defines the critical temperature where magnetization changes from ferrimagnetic to superparamagnetic. Naturally, if superparamagnetic magnetism dominates at room temperature, the effective Curie temperature of magnetite nanoparticles (738 K) must be lower. Indeed, the higher proportion of surface spins in nano-scale particles enhances the dipolar anisotropy, lowering the Curie temperature (temperature at which single-ion and dipolar anisotropy terms are equivalent) (Thapa *et al*., 2004).

Saturation magnetization in nano-scale magnetite particles follows two distinct patterns as particle size decreases. EPMA analyses suggest that particle size reduction spurs relative oxygen concentration decline, causing slight reduction in iron valence states (Thapa *et al*., 2004). This scenario generates greater ferrous ion content; since the ultimate magnetic moment depends upon ferrous species, subsequent increase in magnetization should be observed. Magnetization varies along particle diameter with greater magnitude within the particle and lower magnitude near the surface. Therefore, as particle diameter is decreased, surface effects will eventually affect saturation magnetization. Researchers have discovered that below 10 nm, saturation magnetization suddenly reversed trend and began decreasing with particle size (Thapa *et al*., 2004). Basically, at extremely small nanoparticle dimensions (diameter < 10 nm), saturation magnetization decreases with decreasing particle size because

surface effects.

In presence of external magnetic field, the induced magnetic field surrounding magnetite nanoparticles is larger than for bulk magnetite (Ebner *et al*., 1997). This beneficial nano-scale property allows for enhanced magnetic separation capabilities (to be discussed in section five).

5 APPLICATIONS

Given magnetite's nano-scale magnetic properties (superparamagnetism), material scientists and electrical engineers may dismiss magnetite as being a meaningless venture. Contrarily, environmental, chemical, and biological engineering engineers may take different stances on the matter. Opportunities for magnetite nanoparticles to be effectively incorporated into environmental contaminant removal and cell separation (Honda *et al*., 1998; Ebner *et al*., 1999; Rikers *et al*., 1998; Navratil, 2003), magnetically guided drug delivery (Roger *et al*., 1999), magnetocytolysis (Roger *et al*., 1999), sealing agents (liquid O-rings) (Enzel *et al*., 1999), dampening and cooling mechanisms in loudspeakers (Enzel *et al*., 1999), and contrasting agents for magnetic resonance imaging (MRI) (Schütt, 2004). Advancement of synthesis and stabilization procedures towards production of uniformly sized, dispersed (potentially embedded) magnetite nanoparticles has clearly inspired creative imagination and application in various fields. The following subsections address the topics mentioned above towards understanding of the capabilities offered by magnetite nanoparticles.

5.1 High Gradient Magnetic Separation

High gradient magnetic separation (HGMS) techniques involving magnetite nanoparticles have abounded over the past decade. HGMS, as the name implies, involves magnetic

separation of suspended particles. One evident employment of this technology involves implementation of magnetite nanoparticle generated HGMS-effect towards traditional water treatment plant coagulation needs. Basically, magnetite nanoparticles act as magnetic seeding agents, eventually forming magnetically active flocs with other suspended particles (suspended solids, bacteria, plankton) (Kurinobu *et al*., 1999). The magnetite nanoparticles present in these flocs can be effectively recovered, separated, and reutilized. Such sustainable employment has many advantages over typical water treatment residuals: decreased sludge generation, reduced sludge transport and disposal costs, and diminished virgin coagulant demands. Research studies demonstrate practical recovery and reutilization of magnetite particles in coagulation operations; 100% of magnetite particles present in water treatment residuals, 95% of magnetic particles subsequently recovered from the sludge (Kurinobu *et al*., 1999).

Drinking water requirements mandate colloidal particle (including bacterium, solids, etc.) removal. These particles are typically removed via introduction of iron(III) or aluminum(II) salts, which attract negatively charged suspended particles generating flocculation, to the water column. Particle mass eventually surpasses the colloidal regime, allowing for gravity-induced settling. The proposed HGMS technique follows similar process dynamics as outlined below and illustrated in Figure 12. The open literature has documented the adsorptive properties of magnetite extensively (Ebner *et al*., 1999; Navratil, 2003; Honda *et al*., 1998; Kurinobu *et al*., 1999). Therefore, negatively charged ligands, electrolytes, and other suspended particles will undergo interaction (adsorption) with magnetite's active surface sites. Ultimately, the size of magnetically active flocs will allow gravitational

forces (settling forces) to exceed Brownian motion (suspension forces), producing sludge at the reactor bottom. These water treatment residuals (i.e., sludge) are collected and submitted to an HGMS-system, permitting magnetite nanoparticle recovery and subsequent reuse.

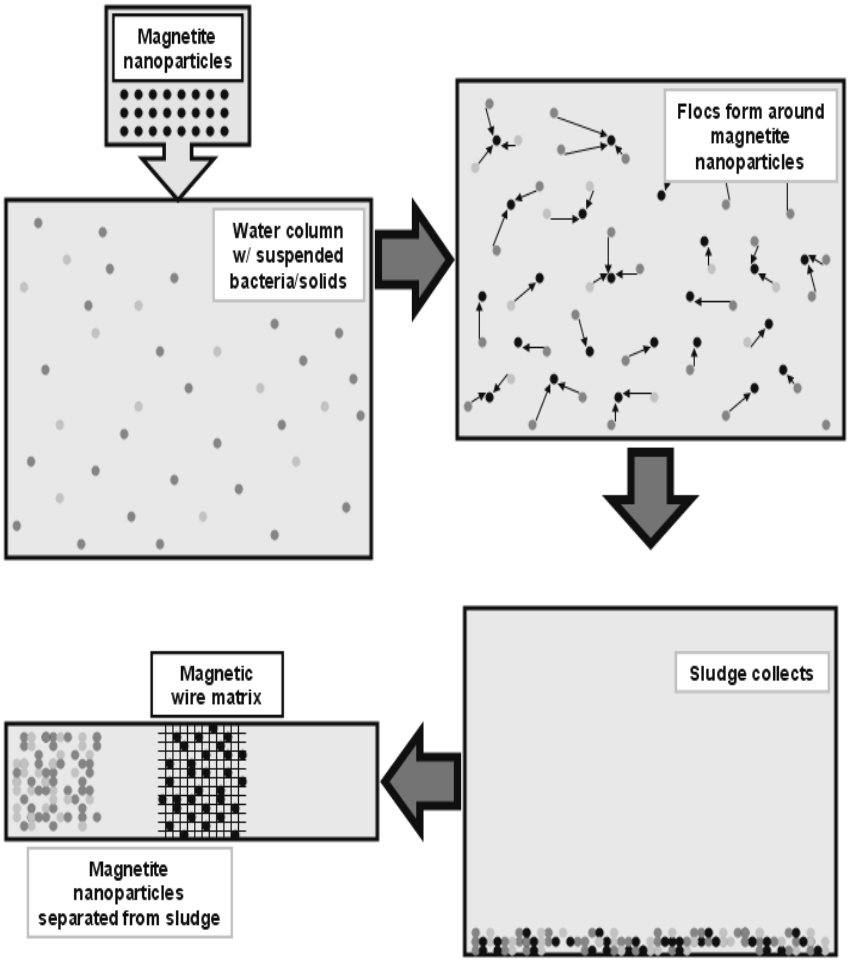

Figure 12. Magnetite coagulant utilization through HGMS technique

Another environmental HGMS application of magnetite nanoparticles involves the wastewater treatment industry. Following treatment of wastewater, bio-solids must be separated from treated water; this procedure is often completed through filtration or clarification techniques. These technologies, while efficient, have inherent disadvantages such as pressure drop, long retention times, and large reactor volumes. Again, magnetite nanoparticles will be utilized as coagulant; however, much higher bio-solid concentrations are now present. Recent research demonstrates greater than 90% *Escherichia coli* cell recovery in activated sludge-like systems (Honda *et al*., 1998).

Another HGMS-oriented environmental approach involves utilization of polymeric resins impregnated with magnetite nanoparticles (recall the copolymer gel synthesis procedure discussed in section three) towards removal of hazardous wastes from aqueous systems. Like most iron oxides, activated magnetite nanoparticles offer impressive adsorption capabilities; however, problems associated with pressure-drop prohibit magnetite nanoparticle utilization in plug-flow (columnar) reactors. This predicament is overcome through effectively loading magnetite nanoparticles into polymeric resins. The resultant hybrid material exhibits structural rigidity and strength of micro-scale polymeric resins and adsorptive properties of nano-scale magnetite. Superparamagnetic behavior of magnetite nanoparticles (discussed in section four) facilitates in adsorption and retention of target species; superparamagnetic magnetization also allows for HGMS-recovery of magnetite nanoparticles to be realized. Monodispersed magnetite nanoparticles that are surface-coupled towards treatment of specific species have been widely utilized in HGMS (Schütt, 2004); furthermore, this coating prevents magnetite oxidation to maghemite (Kiely,

2006).

One commonly employed application of this technology is removal of actinides from wastewater streams. Actinides are highly toxic, radioactive elements present in nuclear wastes. The actinide class (periodic table's last row) includes elements ranging from atomic number ninety (thorium) to one hundred and three (lawrencium); elements commonly found in nuclear waste streams include uranium, neptunium, plutonium, and americium. Researchers have found that hybrid magnetite-polymeric resin particles exhibited greater treatment capacity than both conventional ferric oxide surface complexation adsorption processes and also traditional HGMS technologies (Ebner *et al*., 1999).

Nano-scale magnetite provides metal ion adsorption, HGMS, or both, depending on the waste stream characteristics (Navratil, 2003). For those reasons, great potential for magnetite nanoparticle employment towards treatment and recovery of various heavily contaminated waste streams exists (Rikers *et al*., 1998). In fact, Dr. Arup SenGupta of the Lehigh University Civil and Environmental Engineering department plans on investigating the capability for magnetite nanoparticle embedded ion exchange resins towards remediation of arsenic contaminated waters in the near future.

5.2 Ferrofluids

Ferrofluids are colloidal suspensions containing nano-scale magnetite particles; in the presence of strong magnetic fields, the ferrofluid will grow "spikes" along magnetic field lines. The photograph on the cover of this report illustrates ferrofluid physico-morphosis under magnetic field influence; Figure 13 further demonstrates ferrofluid physico-morphosis.

In conclusion, ferrofluids are *really* cool! However, in addition to being amazing material science artwork,

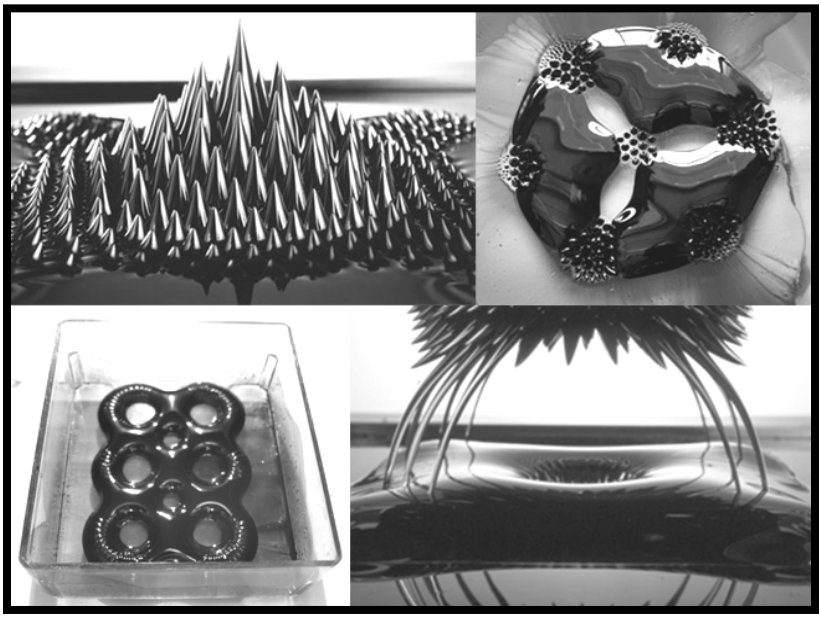

Figure 13. Ferrofluid physico-morphosis under magnetic field

ferrofluids have many unique properties and potential applications. Descriptions of ferrofluid implementation into various technologies are presented in the sections below.

5.2.1 Magnetic Resonance Tomography

Magnetic Resonance Tomography (MRT) permits non-invasive visualization of cross-sectional images of the human body, tissues, and organs (Schütt, 2004). The MRT technique provides better tissue resolution than traditional radiation based technologies; with addition of contrasting agents, this resolution can be further enhanced (Shao *et al*., 2005). Magnetite nanoparticles (in ferrofluid form) are powerful contrasting agents due to their paramagnetic magnetization, as demonstrated in Figure 14.

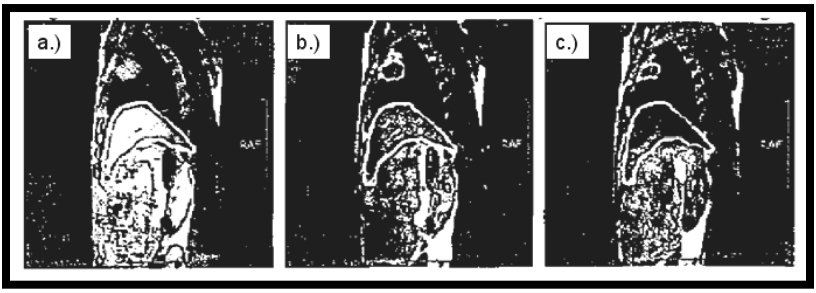

Figure 14. Time1 (T1) and Time2 (T2) magnetic resonance images of the liver of rabbit before and after injecting contrast agent: (a) T1 image before injecting (b) T2 image of before injecting (c) T2 image after injecting (Shao et al., 2005)

Human bloodstreams readily reject the nanoparticle colloidal solution, which quickly passes into the liver (Shao *et al*., 2005). Consequently, ferrofluids have thus far only been useful in distinguishing between healthy and malignant liver cells. This limitation can be overcome through functionalization of magnetite nanoparticles with various ligands allows for organ-specific transport; therefore, MRT imaging of various bodily organs can be possible. Furthermore, polymeric (i.e., polyethylene oxide - PEO) coating of functionalized magnetite particles permits ferrofluids longer bloodstream retention. (Schütt, 2004)

PEO coatings are applied through magnetite interaction with copolymer PEO-polypeptide; polypeptides interact with the positively charged magnetite surface and provide nanoparticle masking to allow longer bloodstream residence. These coated magnetite nanoparticles could also be employed as extremely efficient capsules for drug delivery systems, which will be discussed below. (Schütt, 2004)

5.2.2 Magnetically Guided Drug Delivery

Ferrofluids containing encapsulated (with biologically compatible surface chemistries) magnetite nanoparticles, as described above, can be employed for drug delivery to specific locations. Exploitation of superparamagnetic magnetization of magnetite nanoparticles allows for "magnetic dragging" of internal (present in bloodstream or elsewhere) magnetite nanoparticles carrying DNA, enzymes, drugs to target-areas. Similarly, biological effectors, which are proteins (containing DNA specific to target cells) incorporated into encapsulated nanoparticle surface functionality, allow for target cell specificity. Once biological effector carrying magnetic nanoparticles bind to target-cells, the applied magnetic field is fluctuated (approximately 1 MHz) causing magnetocytolysis, or cell destruction, which eliminates target-cells. Similarly, after being dragged to target areas, magnetocytolysis of encapsulated nanoparticles can release drugs. Research towards these ends is currently being heavily investigated as potential for novel drug/cancer treatment abounds. (Roger *et al*., 1999)

5.2.3 Mechano-Electrical Applications

Ferrofluids have some very interesting potential applications in various mechanical/electrical situations. Rotating shafts protruding into low- or high-pressure chambers oftentimes exert a great deal of friction on traditional rotating mechanical seals (commonly known as O-rings). Such seals are employed in rotating anode x-ray generators and vacuum chambers operated by the semiconductor industry. Ferrofluid seals secured with permanent magnets provide firm seals with minimal friction. (Enzel *et al*., 1999)

Another novel application of ferrofluids allows

improved performance of loudspeakers. Electric energy in loudspeakers is delivered through coils situated in the center of permanent circular magnets. The resultant magnetic field generates vibrations, which consequently produce sound and thermal energy. Through exploitation of the circular magnet's presence, the coil can be suitably (permanently) coated with ferrofluid, which subsequently provides sound dampening and cooling mechanisms. (Enzel *et al*., 1999)

5.3 Potential Applications

While completing the many (countless!) hours of research necessary for this report, various potential applications of ferrofluids in the environmental engineering field (and others) surfaced in my mind. The maximum word count is rapidly approaching; therefore, *summarized* thoughts are recorded below.

- Magnetically active membrane biological reactor (MBR); magnetic water treatment residuals allow for traditional MBR wasting difficulties to be overcome (such a promising idea!).

- Non-alkaline/non-acidic regenerant solution for regeneration of exhausted adsorptive/ion-exchange media.

- Effective recovery of hazardous wastes in extremely concentrated volumes.

- Microfluidic applications; currently much research effort surrounds controlled flow of microfluids. Ferrofluids appear to have great potential as they effectively carry and transport DNA, enzymes, and other biomolecules.

6 CONCLUSION

Bulk and nano-scale properties of magnetite have been documented and discussed; methods of synthesizing magnetite nanoparticles have been described at length; potential applications and markets for novel employment of nano-scale magnetite have been explored. An ancient proverb states, "One man's trash is another man's treasure." That proverb definitely applies to magnetite nanoparticles. Recently in class, Dr. Kiely stated that at high temperatures ferromagnetic particles exhibit superparamagnetic behavior, and *then they are worthless*. Perhaps, such particles are worthless for materials science and electrical engineering applications (hence the lack of depth in the nano-scale electrical properties section); however, superparamagnetic behavior allows for some very interesting environmental, chemical, and biological engineering applications. Novel ideas for magnetite nanoparticle incorporation are being rapidly processed in engineering fields (even by myself!). Undoubtedly, the times are extremely conducive and exciting for engineers delving into the nano-world. Thank you, Dr. Kiely, for assigning this essay assignment, potential realization of the nano-scale magnetite enhanced membrane bioreactor wasting procedure, mentioned in section five, is a likely byproduct.

Works Cited

Bellis M (2006). Magnetic compass. Inventors.com <http://-inventors.about.com/library/inventors/blcompass.htm>

Blakemore RP (1982). Magnetotactic bacteria. *Annu. Rev. Microbiol*. 36:217-238

Breulmann M, Colfen H, Hentze HP, Antonietti M, Walsh D, Mann S (1998). Elastic magnets: template-controlled mineralization of iron oxide colloids in a sponge-like gel matrix. *Adv. Mater*. 10, 237-241

Cornell RM and Schwertmann U. *The iron oxides*. VCH Press, Weinheim, Germany, 1996

Ebner AD, Ritter JA, and Ploehn HJ (1997). Feasibility and limitations of nanolevel high gradient magnetic separation. *Separation and Purification Technology*, 11, 199-210

Ebner AD, Ritter JA, Ploehn HJ, Kochen RL, and Navratil JD (1999). New magnetic field-enhanced process for the treatment of aqueous wastes. *Separation Science and Technology* 34, 1277-1300

Enzel P, Adelman N, Beckman KJ, Campbell DJ, Ellis AB, Lisensky GC (1999). Preparation of an aqueous-based ferrofluid. *J. Chem. Educ*. 76, 943-948

Fried T, Shemer G, Markovich G (2001). Ordered two-dimensional arrays of ferrite nanoparticles. *Adv. Mater*. 13, 1158-1161

Hill RJ, Craig JR, and Gibbs GV (1979). Systematics of the spinel structure type. *Physics and Chemistry of Minerals*, 4, 317-339

Hemingway BS (1990). Thermodynamic properties for bunsenite, NiO, magnetite, Fe_3O_4 and hematite, Fe_2O_3 with comments on selected oxygen buffer reactions. *American Mineralogist* 75, 781-790

Honda H, Kawabe A, Shinkai M, and Kobayashi T (1998). Development of chitosan-conjugated magnetite for magnetic cell separation. *Journal of Fermentation and Bioengineering* 86, 191-196

Hou YL, Yu JF and Gao S (2003). Solvothermal reduction synthesis and characterization of superparamagnetic magnetite nanoparticles. *J. Mater. Chem.* 13, 1983-1987

Kang YS, Risbud S, Rabolt JF, and Stroeve P (1996). Synthesis and characterization of nanometer-size Fe_3O_4 and y-Fe_2O_3 particles. *Chem. Mater*. 8, 2209-2211

Kiely CH (2006). Materials for nanotechnology notes

Kim DK, Zhang Y, Voit W, Rao KV, and Muhammed M (2001). Synthesis and characterization of surfactant-coated superparamagnetic monodispersed iron oxide nanoparticles. *Journal of Magnetism and Magnetic Materials* 225, 30-36

Kostov I. Mineralogy. Edinburgh: Oliver & Boyd, 1968

Kurinobu S, Uesugi J, Utumi Y, and Kasahara H (1999). Performance of HGMS Filter and recycling of magnetic seeding material on magnetic seeding method. *IEEE Transactions on Magnetics* 35, 4067-4069

Lee Y, Lee J, Bae CJ , Park JG, Noh HJ, Park JH, and Hyeon T (2005). Large-scale synthesis of uniform and crystalline magnetite nanoparticles using reverse micelles as nanoreactors under reflux conditions. *Adv. Funct. Mater*. 15, 503-509

Lin H, Watanabe Y, Kimura M, Hanabusa K and Shirai H (2003). Preparation of magnetic poly(vinyl alcohol) (PVA) materials by in situ synthesis of magnetite in a PVA matrix. *J. Appl. Polym. Sci.* 87, 1239-1247

Mannweiler U (1966). Vergleich dreier methoden zur bestimmung spezifischer oberflachen von pulvern. *Chimia* 20, 363-364

Massart R (1981). Preparation of aqueous magnetic liquids in alkaline and acidic media. *IEEE Trans. Magn*. 17, 1247-1248

Meisen U and Kathrein H (2000). The influence of particle size, shape and particle size distribution on properties of magnetites for the production of toners. *Journal of Imaging Science and Technology*, 44(6): 508-513

Mills AA (2004). The lodestone: history, physics, and formation. *Annals of Science* 61, 273–319

Morais PC, Garg VK, Oliveira AC, Azevedo RB, Rabelo D, and Lima ECD (2002). Synthesis and characterization of magnetite nanoparticles embedded in copolymer microspheres. *European Cells and Materials* 3, 173-175

Navratil JD (2003). Adsorption and nanoscale magnetic separation of heavy metals from water. U.S. EPA workshop on managing arsenic risks to the environment: characterization of waste, chemistry, and treatment and disposal. Denver, CO

Pawlow P (1909). Uber die abhängigkeit des schmelzpunktes von der oberflächenenergie eines festen körpers. *Zeitschrift fur phys. Chemie* 65, 545

Qu SC, Yang HB, Ren DW, Kan SH, Zou GT, Li DM and Li MH (1999). Magnetite nanoparticles prepared by precipitation from partially reduced ferric chloride aqueous solutions. *J. Colloid Interface Sci*. 215, 190-192

Rabelo D, Lima ECD, Reis AC, Nunes WC, Novak MA, Morais PC (2000). Preparation of magnetite nanoparticles in mesoporous copolymer template. *Nano Letters* 1, 105-108

Rikers RA, Voncken JHL, and Dalmijn WL (1998). Cr-polluted soil studied by high gradient magnetic separation and electron probe. *Journal of Environmental Engineering* 124, 1159-1164

Robie RA, Hemingway BS, and Fisher JR (1979). Thermodynamic properties of minerals and related substances at 298.15 K and 1 bar (10^5 Pascals) pressure and at higher temperatures. *US. Geol. Surv. Bull.* 1452

Roger J, Pons JN, Massart R, Halbreich A, and Bacri JC (1999). Some biomedical applications of ferrfluids. *Eur. Phys. J. AP* 5, 321-325

Sahoo Y, Pizem H, Fried T, Golodnitsky D, Burstein L, Sukenik CN, and Markovich G (2001). Alkyl phosphonate/phosphate coating on magnetite nanoparticles: a comparison with fatty acids. *Langmuir* 17, 7907-7911

Samsonov GV. *The Oxide Handbook* .IFI-Plenum, New York, 1973

Sapieszko RS and Matijevic E (1980). Preparation of well-defined colloidal particles by thermal decomposition of metal chelates. *J. Colloid Interface Sci*. 74, 405-422

Schmidt M, Kusche R, Kronmüller W, von Issendorff B, and Haberland H (1997). Experimental determination of the melting point and heat capacity for a free cluster of 139 sodium atoms. *Physical Review Letters* 79, 99-102

Schütt D (2004). Magnetite colloids for drug delivery and magnetic resonance imaging. Institute Angewandte Polymerforschung: thesis Selim MS, Cunningham LP, Srivastava R, Olson JM (1997). Preparation of nano-size magnetic gamma ferric oxide (γ-Fe_2O_3) and magnetite (Fe_3O_4) particles for toner and color imaging applications. *Recent Progress in Toner Technologies*, 108-111

Seoighe C, Naumann J, and Shvets I (1999). Studies of surface structures on single crystalline magnetite (100). *Surf. Sci.* 440, 116

Shaikhutdinov S and Weiss W (2000). Adsorbate dynamics on iron oxide surfaces studied by scanning tunneling microscopy. *Journal of Molecular Catalysis A: Chemical* 158, 129-133

Shao H, Lee H, Huang Y, Kwak BK, and Kim CO (2005). Synthesis of nano-size magnetite coated with chitosan for MRI contrast agent by sonochemistry. *Magnetics Conference, 2005. INTERMAG Asia 2005. Digests of the IEEE International*, 461-462

Suber L, Foglia S, Ingo GM, and Boukos N (2001). Synthesis, and structural and morphological characterization of iron oxide-ion-exchange resin and -cellulose nanocomposites. *Applied Organometallic Chemistry* 15, 414–420

Sun SH and Zeng H (2002). Size-controlled synthesis of magnetite nanoparticles. *J. Am. Chem. Soc*. 124, 8204-8205

Sweeton FH and Baes CF (1970). The solubility of magnetite and hydrolysis of ferrous ion in aqueous solutions at elevated temperatures. *J. Chem. Thermodyn*. 2, 479-500

Tang J, Myers M, Bosnick KA, Brus LE (2003). Magnetite Fe_3O_4 nanocrystals: spectroscopic observation of aqueous oxidation kinetics. *J. Phys. Chem. B* 107, 7501

Tartaj P and Serna CJ (2002). Synthesis of monodisperse superparamagnetic Fe/silica nanospherical composites. *Chem. Mater*. 125, 15754-15755

Thapa D, Palkar VR, Kurup MB, and Malik SK (2004). Properties of magnetite nanoparticles synthesized through a novel chemical route. *Materials Letters* 58, 2692-2702

Visalakshi G, Venkateswaran G, Kulshreshtha SK, and Moorthy PH (1993). Compositional characteristics of magnetite synthesized from aqueous solution at temperatures up to 523 K. *Mat. Resource Bull*. 28, 829-836

Weidenfeller B, Höfer M, Schilling F (2002). Thermal and electrical properties of magnetite filled polymers. *Composites Part A: Applied Science and Manufacturing* 33, 1041-1053

Woo K, Hong J, Choi S, Lee HW, Ahn JP, Kim CS, and Lee SW (2004). Easy synthesis and magnetic properties of iron oxide nanoparticles. *Chem. Mater*. 16, 2814-2818

Zhou ZH, Wang J, Liu X, Chan HSO (2001). Synthesis of Fe_3O_4 nanoparticles from emulsions. *J. Mater. Chem*. 11, 1704-1709

Figures Cited

Figures 1, 4-9, and 12 all by Lee Blaney

Figure 2: <http://www.ifm.eng.cam.ac.uk/people/sc444/images/2a_200_167.jpg>

Figure 3: <http://www.soes.soton.ac.uk/resources/collection-/minerals/minerals/images/M08-Magnetite.jpg

Figure 10: <http://www.ndt-ed.org/EducationResources/CommunityCollege/MagParticle/Graphics/BHCurve.gif

Figure 11: <http://www.chem.pku.edu.cn/mmm/doc/publications/J-Mat-Chem/HouYL-Fe3O4.pdf

Figure 13: <http://www.projectarcanum.com/wp-content/uploads/2006/01/photo01_1.jpg>; <http://userwww.sfsu.-edu/~infoarts/links/artsciencelecture/physic.art/frankel.ferrofluid.ff.jpg>; <http://www.ian.org/Magnetics/Small-RingsFerrofluid.JPG>; <http://roclar.net/RP/Kodama-Ferrofluidsculptures.jpg>

Figure 14: <http://ieeexplore.ieee.org/iel5/9890/31427/-01463659.pdf?isnumber=&arnumber=1463659>

Appendix A: Spreadsheet of Magnetite Properties

Property	Value	Details
bandgap	0.1 eV	almost semi-conductor
boiling point	2623 °C	
cleavage	none	
coercivity (bulk-scale)	2.4-20.0 kA/m	coercivities are in range of disk-drive recording media and permanent magnets
coercivity (nano-scale)	0	superparamagnetic
color (bulk-scale)	black	
color (nano-scale)	black	suspended solutions of magnetite nanoparticles exhibit jet black color
conductivity	10^2-10^3 /Ω/cm	almost metallic
conductivity exchange constants	high	electrons are thermally delocalized over Fe^{2+} and Fe^{3+} ions
JAA	-18 J·K	
JAB	-28 J·K	
JBB	3 J·K	
crystal structure	inverse spinel	alternating octahedra and tetrahedra-octahedral layers
Curie temperature (bulk-scale)	850 K	below Tc - spins on tetrahedral sites occupied by Fe^{3+} and octahedral sites occupied by Fe^{2+} and Fe^{3+} are anti-parallel
Curie temperature (nano-scale)	738 K	higher proportion of surface spins in nano-scale particles enhances the dipolar anisotropy
density	5.18 g/cc	
dissolution behavior	fast	faster than pure ferric oxides

electrical properties	between metal and semi-conductor	slightly metal deficient with vacancies on octahedral sites n and p type semiconductorband gap = 0.1 eV - lowest resistivity of any oxide conductivity = 10^2-10^3 /Ω/cm - almost metallic good conductivity due to closeness of Fe^{2+} and Fe^{3+} ions on octahedral sites
forms	{111}	4 threefold axes
formula	Fe_3O_4	
formula units/unit cell	z = 8	
hardness	5.5	
heat capacity function	$Cp = 2659.108 - 2.52153 \cdot T + 1.36769 \cdot 10^{-3} T^2 - 3.645541 \cdot 10^4 T^{-0.5} + 2.07344 \cdot 10^7 T^{-2}$	between 290-800 K
heat of decomposition	605 kJ/mol	
heat of fusion	138.16 kJ/mol	
heat of vaporization	298 kJ/mol	at 2623 °C
infrared bands	580 and 400 /cm	surface OH groups
lattice parameter (bulk-scale)	a = 8.39 Å	
lattice parameter (nano-scale)	a = 8.40 Å	due to Laplace pressure
magnetic properties (bulk-scale)	ferrimagnetic	can produce magnetites with coercivities between 2.4-20 kAm-1 by controlling precipitation
magnetic properties (nano-scale)	superparamagnetic	
melting point (bulk-scale)	1583-1597 °C	

melting point (nano-scale)	<1583 °C	due to inverse relationship between melting point and particle diameter as stated by Pawlow; necessary variables were not available to compute the nano-scale melting point
morphology	octahedral crystals	bounded by {111} planes and rhombo-dodecahedra
parting	along {111}	
porous	not porous	
saturation magnetization (bulk-scale)	2.0 μ_B/fu	for 91.4nm diameter particle
saturation magnetization (nano-scale)		relative oxygen concentrations decline causing valence states of iron cations to be slightly reduced, generating greater ferrous ion content; since the ultimate magnetic moment depends upon ferrous species, subsequent increase in magnetization; below 10 nm surface effects cause saturation magnetization to decrease
particle size	6.4 nm	1.1 μ_B/fu
	10.8 nm	2.6 μ_B/fu
	37.8 nm	2.3 μ_B/fu
solubility	$K_{so} = 12.02$	for the reaction: $(1/3)Fe_3O_4 + 2H^+ + (1/3)H_2 = Fe^{2+} + (4/3)H2O$
solubility product	35.7	from $\log(Fe^{2+})^3/(H)^8.(e^-)^2$
Standard free energy of formation	-1012.6 kJ/mol	

structure	inverse spinel	due to crystal field stabilization energy (CFSE) greater in Fe^{2+} for octahedral than tetrahedral coordination so Fe^{2+} occupies octahedral sites - Fe^{3+} CFSE is zero, so no preference
surface area (bulk scale)	6 m^2/g	for 200nm diameter particle
surface area (nano-scale)	100 m^2/g	for 50nm diameter particle
terracing	present	cubic terracing occurs on the (100) face; atomically flat terracing, oriented along the main crystallographic direction, occurs on the (111) plane
twinning	occurs on {111} plane	
unit cell	face-centered cubic	
unit cell volume (bulk-scale)	592.7 $Å^3$	
unit cell volume (bulk-scale)	590.6 $Å^3$	due to Laplace pressure

Appendix B: Other Nanoparticle Synthesis Techniques

Although the literature describes numerous techniques to synthesize magnetite nanoparticles, this report only details the theory and process dynamics for those listed above. Some other synthesis methods available through the literature include solvothermal reduction and thermal decomposition (Hou *et al.*, 2003; Sapieszko and Matijevic, 1980; Woo *et al.*, 2004; Sun and Zeng, 2002).

- Solvothermal Reduction –involves reduction of ferric species (ferric acetylacetonate) in the presence of steric stabilizing surfactants within alcohol (ethylene glycol)

by a strong reducing agent (hydrazine). Size control was achieved through the surfactant molecule utilized, precluding highly efficient production of uniformly sized nanoparticles across wide-ranging diameter dimensions. (Hou *et al*., 2003; Sapieszko and Matijevic, 1980)

- Thermal Decomposition – concerns ferrate (Fe^{5+}) species (iron pentacarbonyl) reduction in the presence of stabilizing surfactant molecules within ether solution (octyl ether) at 100 °C temperature. Ensuing ferrate mixing with ether and surfactant solutions, heating and refluxing of the solution occurs until solution color transitions from colorless to black. This solution was then allowed to cool; subsequently, magnetite nanoparticles were recovered through centrifugation with ethanol. Nanoparticle size is controlled by varying concentrations (molar ratio) of ferrate to surfactant. (Woo *et al*., 2004; Sun and Zeng,, 2002)

The two alternate synthesis procedures mentioned above are oftentimes slightly altered depending on the researcher performing the reaction. Given procedures vary because each technique has unique advantages/disadvantages related procured resources and intended application of magnetite nanoparticles; however, general procedures were given to highlight the methods and concepts associated with the given principle.